Journal of Electroanalytical Chemistry 875 (2020) 113862

Contents lists available at ScienceDirect

Journal of Electroanalytical Chemistry

journal homepage: www.elsevier.com/locate/jelechem

Highly dispersed, single-site copper catalysts for the electroreduction of CO_2 to methane

Teng Zhang [a], Sumit Verma [b,c], Soojeong Kim [d], Tim T. Fister [d], Paul J.A. Kenis [b,c], Andrew A. Gewirth [a,c,*]

[a] Department of Chemistry, University of Illinois at Urbana-Champaign, Urbana, IL 61801, USA
[b] Department of Chemical & Biomolecular Engineering, University of Illinois at Urbana-Champaign, Urbana, IL 61801, USA
[c] International Institute for Carbon Neutral Energy Research (WPI-I2CNER), Kyushu University, Fukuoka, Japan
[d] Chemical Sciences and Engineering Division, Argonne National Laboratory, Argonne, IL 60439, USA

ARTICLE INFO

Article history:
Received 27 September 2019
Received in revised form 9 December 2019
Accepted 15 January 2020
Available online 16 January 2020

Keywords:
CO_2 electroreduction
Single-site catalysts
Copper
Methane

ABSTRACT

Pyrolyzing Cu(II) precursors absorbed on carbon black gave an eletrocatalytic material for the electroreduction of CO_2. Controlled potential electrolysis and GC analysis revealed an unexpected selectivity towards methane even in alkaline media, with a methane Faradaic efficiency as high as 42%, a partial current density of 100 mA/cm^2 (at −1 V vs. RHE) and a methane/ethylene ratio of 4:1. XPS, EXAFS, and EDX mapping results indicate a single-site Cu(I) center as the catalytically active site. The limited size of the active sites is believed to be crucial for the preferential formation of methane over ethylene.

The atmospheric CO_2 concentration reached 400 ppm in the year 2016, for the first time since recording began [1]. Global warming and resulting effects such as melting ice caps and increasingly erratic weather patterns have been linked to the rapidly using atmospheric CO_2 levels [2]. Converting CO_2 into useful molecules or materials has been proposed as a promising and potentially economically feasible approach to reduce CO_2 emissions by using it as a feedstock for intermediates such as CO and ethylene for carbon chemical and fuel production. [3,4] The renewable electricity-driven electroreduction of CO_2 could be one approach for CO_2 utilization, and has attracted great research interest in recent years. However, challenges remain in seeking electrocatalysts with low cost, high activity and desired selectivity. Depending on the catalyst used, the electroreduction of CO_2 produces different combinations of C1 and C2 products, such as CO, formate, methanol, methane, ethylene, ethanol, and acetate. [5–7] Moreover, the electroreduction CO_2 in aqueous media also competes with the hydrogen evolution reaction (HER), as this reaction occurs at a similar reduction potential. The choice of an electrode material or electrocatalyst will be crucial for producing different products, ideally selectively.

Metallic Cu is one of the few electrode materials that prefers CO_2 reduction over the HER, and the only one known to produce appreciable amounts of hydrocarbons upon CO_2 reduction [8,9]. Scientists have investigated a variety of copper-based electrocatalysts for CO_2 reduction, from metallic nanoparticles [10–18], alloys and bimetallic composites [19–27], oxides [28–30], to molecular complexes [31–33]. Recently, single-atom catalysts (SACs) attract great interest in electrochemical energy conversion [34,35], yet not many copper-based SACs are reported. Use of bulk polycrystalline metallic copper electrodes usually produces C_2H_4 [9,36–40], but some selectivity for methane was also reported [8]. Changing the size [12,14], morphology [15,17,41], or surface modification [42–44] of metallic Cu can change product selectivity. Molecular Cu complexes tend to selectively produce CO in non-aqueous solution [31], yet uncommon products such as oxalate or methyl formate have been reported as well [32,45]. The choice of electrolyte, pH, and solvent also affects product distribution [39,46].

With Cu-based electrodes or electrocatalysts, ethylene is usually the more preferred product under alkaline conditions (high pH) [47]. Despite the many reports, selective production of methane is quite uncommon. Methane has been reported as the major product when electrolysis takes place at a lower temperature such as 0 °C, yet its production is greatly suppressed as temperature increases [9,36]. Selective methane production has been reported on specific crystal faces of Cu single crystal electrode [48–50], a nano-Cu/glassy carbon catalyst [11], polymer-supported CuPd nanoalloys [24], or Cu-porphyrin complexes [33]. However, the preparation of these catalysts requires complicated steps, making them hard to scale up. The current densities obtained were also limited due to small surface areas of the material as well as low CO_2 solubility in the aqueous electrolytes used.

Herein we report a CuN composite catalyst embedded in a carbon matrix which is selective for the production of methane via the

* Corresponding author at: Department of Chemistry, University of Illinois at Urbana-Champaign, Urbana, IL 61801, USA.
E-mail address: agewirth@illinois.edu. (A.A. Gewirth).

http://dx.doi.org/10.1016/j.jelechem.2020.113862

Table 1
Synthetic conditions and Cu contents of the catalysts.

Sample	Cu/AHP/carbon feed (mmol/mmol/mg)	Pyrolysis temperature (°C)	Cu wt% by ICP
Cu-N-5%-RT	0.2/0.4/100	N/A	4.1%
Cu-N-5%-400	0.2/0.4/100	400	4.6%
Cu-N-5%-600	0.2/0.4/100	600	4.8%
Cu-N-8%-400	0.4/0.8/100	400	8.3%
Cu-N-13%-400	0.4/0.8/50	400	13.6%

electroreduction of CO_2. By using a gas diffusion electrode in a flow cell setup, we achieved a partial current density of ~100 mA/cm^2 at −1 V vs. RHE for methane production, which is among the highest for Cu-based electrodes and electrocatalysts.

The composite catalyst was prepared in a two-step procedure. First, copper perchlorate, 3-amino-5-hydroxypyrazole (AHP), and carbon black (Vulcan XC72R) were mixed in a solution of methanol and water (4:1 v:v) and stirred overnight. The mixture was then centrifuged, and then the solid was washed, dried, and pyrolyzed at 400 or 600 °C under N_2 for 1 h. Elemental analysis revealed a weight percentage of Cu between 4.6% and 13.6% depending on the feed ratio of the Cu source and carbon black (Table 1). PXRD analysis showed only a broad background signal associated with graphitic carbon for the 400 °C sample, while after 600 °C pyrolysis characteristic peaks for metallic Cu and Cu_2O start to appear (Figs. 1 and S1). TEM images of Cu-N-5%-400 further showed no observable metal or metal oxide nanoparticles (Fig. 1). These results indicate that no Cu metallic or oxide particles formed during pyrolysis at 400 °C (a result strongly supported by EXAFS analysis reported below), and that at higher temperature Cu metal starts to form.

Fig. 2 shows the XPS spectra of the composites after pyrolysis. In the 400 °C material Cu-N-5%-400, the Cu $2p_{1/2}$ and Cu $2p_{3/2}$ peaks appear at binding energies of 952.4 eV and 932.6 eV, respectively, consistent with a Cu oxidation state of 0 or 1. The presence of low oxidation state Cu species is not surprising in these composite materials due to the high temperature and inert atmosphere during pyrolysis. Fitting the Cu 2p peaks uncovers a small contribution (17%) of Cu(II) species, which can be attributed to incomplete reduction or surface re-oxidation when exposed to air. The Cu LMM Auger peaks appear at a kinetic energy of 915.5 eV that can be uniquely assigned to a Cu(I) species (Fig. S2). The unpyrolyzed precursor Cu-N-5%-RT, on the other hand, consists of a mixture of Cu(I) and Cu(II) complexes as indicated by XPS (Fig. 2e and Table 2). The 600 °C material Cu-N-5%-600 shows similar XPS spectra as the Cu-N-5%-400 sample. The N 1 s XPS peaks of pyrolyzed samples can be deconvoluted into two major components (Fig. 2) that corresponded to pyrrolic and pyridinic nitrogen environments, respectively [51]. Majority of nitrogen in pyrolyzed materials adopts in pyridinic functionality. For the unpyrolyzed Cu-N-5%-RT, significant contribution from pyrrolic nitrogen and metal-N species is observed. The XPS data thus indicates partial decomposition of AHP ligand in the composite material.

Electrochemical reduction of CO_2 was carried out in a flow cell similar to that used in our previous work [26,41]. We used 1 M KOH as the electrolyte to increase conductivity, lower overpotential, and suppress H_2 evolution. An IrO_2-coated carbon paper-based gas diffusion electrode was used as the anode to accommodate high current densities. Fig. 3 shows the Faradaic efficiencies (FE) and partial current densities for different reduction products (CO, CH_4, and C_2H_4). A Cu loading as low as 0.06 mg/cm^2 was achieved when depositing Cu-N-5%-400 on a carbon-based gas diffusion electrode (GDE). This sample catalyzes CO formation in the low overpotential region at ~−0.4 V vs. RHE, and the rate increases at more negative overpotentials. However, the Faradaic efficiency for CO production decreases at higher overpotential. At these higher overpotentials, methane and ethylene start to be the dominant products with the total FE for hydrocarbons reaching a maximum of 45–50% at −0.9 to −1.0 V vs. RHE. The Cu-N-5%-400 catalyst also exhibits a methane production FE up to 42% at a partial current density of ~100 mA/cm^2 (corresponding to ~1660 A/g Cu), among the highest current densities reported for Cu-based catalysts to the best of our knowledge (Table S3). The methane/ethylene FE ratio reaches as high as 4:1. However, production of hydrogen still contributes ~20–25% to the total current at quite negative potentials. Use of a GDE covered with the catalyst pyrolyzed at 600 °C (Cu-N-5%-600) does not have a significant effect on production of methane, but results in a slightly higher FE for hydrogen. Using catalysts with higher Cu weight percentage does not have a significant effect on the total current densities. Methane is still the major product, but slightly higher ethylene production efficiencies were observed in the potential range −0.7 to −0.9 V vs. RHE (Fig. S8). In long term experiment, CO_2 reduction activity decreased quickly and hydrogen production became dominant even in a few hours (Fig. 3h).

We compared the composite catalysts against controls such as carbon black and Cu_2O. When carbon black was deposited on a GDE without any copper precursor, the resulting cathode did not show CO_2 reduction activity with CO formation FEs less than 10% and a negligible amount of other C1 and C2 products. A Cu_2O catalyst on a GDE, on the other hand, exhibits good CO_2 reduction activity with C_2H_4 as the major product (Fig. 3d and e), consistent with prior reports [26].

We also compared the catalysts with the unpyrolyzed precursor material Cu-N-5%-RT. The unpyrolyzed material is also a good electrocatalyst for CO_2 reduction but exhibits a lower current density under similar Cu loadings, probably due to less effective electron transfer between the

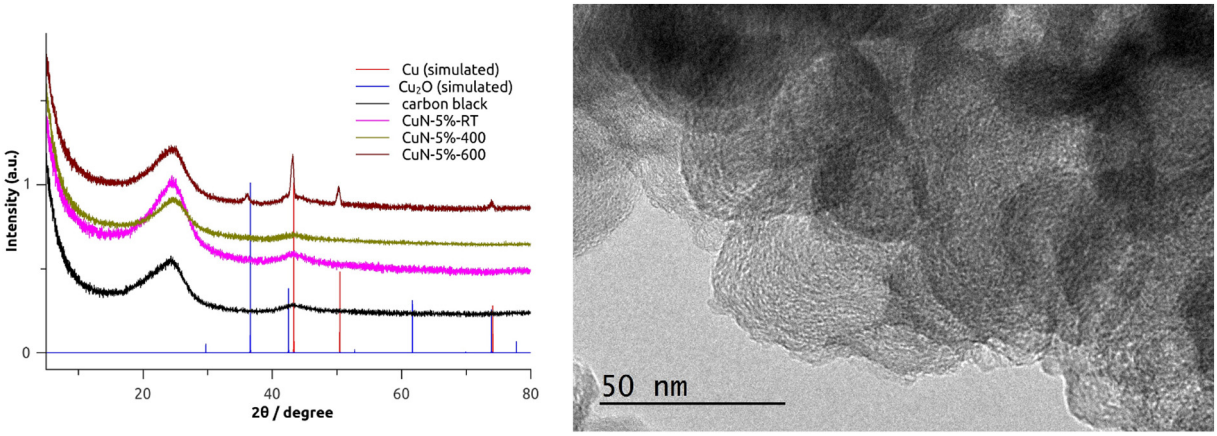

Fig. 1. PXRD patterns of synthesized CuN catalysts (left) and TEM images of Cu-N-5%-400 (right).

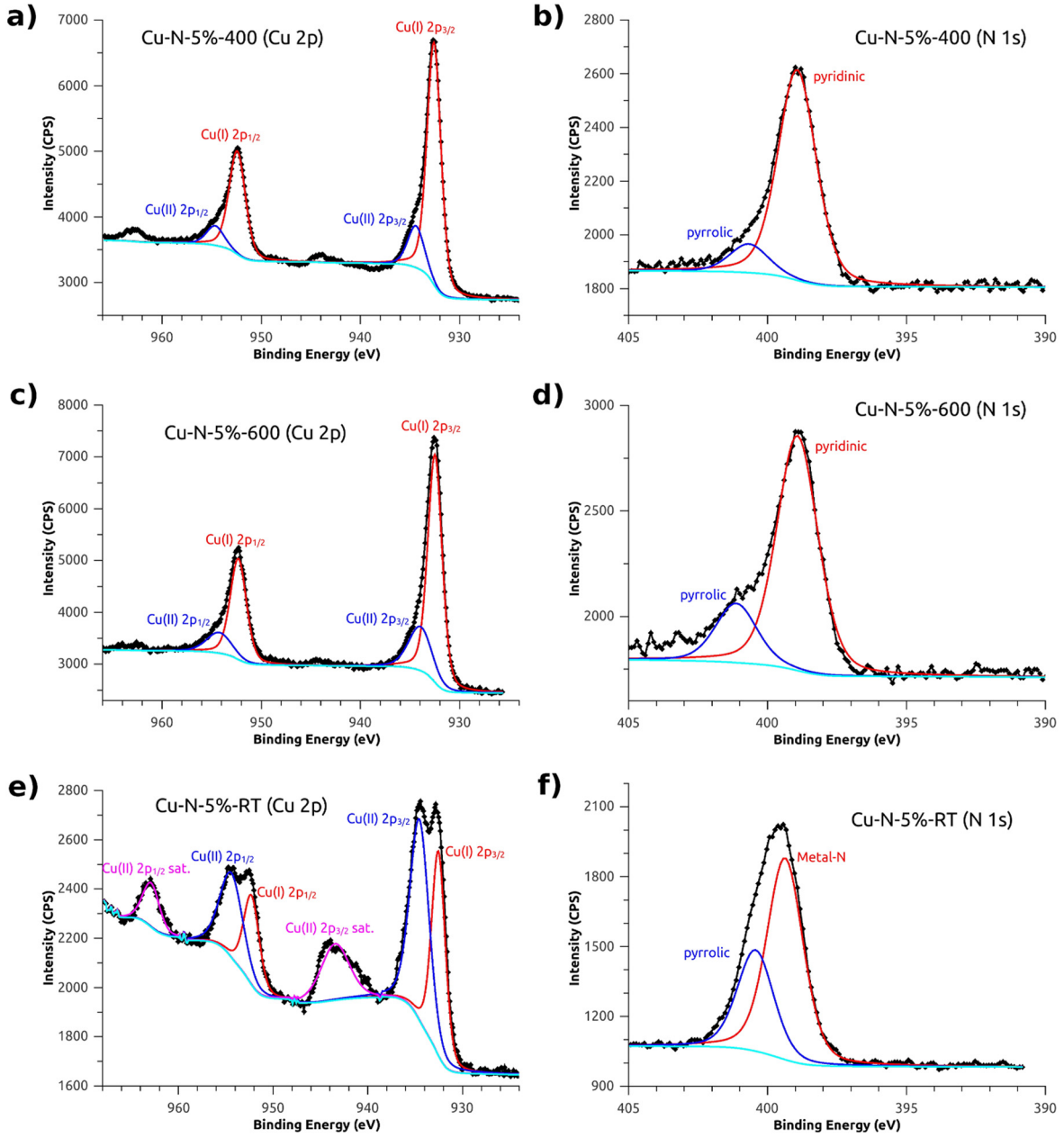

Fig. 2. Cu 2p (a, c, e) and N 1 s (b, d, f) XPS spectra of the CuN catalysts.

carbon matrix and the Cu active site. High FEs for methane and hydrogen were also observed (Fig. 3).

Selectivity for methane is quite uncommon in CO_2 reduction reports, especially in high pH (alkaline) solutions. To understand the structure features of this composite catalyst that would have a strong effect on the product selectivity, we carried out XANES and EXAFS studies on the Cu-N-5%-400 catalyst, as this material exhibited the highest efficiency for methane production. Shown in Fig. 4a, XANES analysis shows that the Cu-N-5%-400 catalyst exhibits a peak at 8982 eV corresponding to the 1s–4s transition of Cu(I) species [52,53]. An additional small peak at 8986 eV for Cu(II) 1s–4s transition shows that a small Cu(II) fraction is also present, consistent with the XPS results. Fig. 4b reports the results of EXAFS obtained from the Cu-N-5%-400 material. Fitting the EXAFS region of the spectrum suggests that the copper center adopts a single-site, four-coordinate environment (Fig. 4). Comparing the R-space spectrum of Cu-N-5%-400 with standard samples Cu_2O and Cu indicates the absence of CuCu scattering paths, suggesting that the Cu center is single site (Fig. S5). We also analyzed the post-electrolysis cathode morphology and elemental distribution of Cu-N-5%-400 by scanning electron microscopy (SEM) and energy dispersive X-ray (EDX) mapping. The SEM images showed no observable metallic particles either before or after electrolysis,

Table 2
Summary of XPS analysis results for CuN catalysts.

Material	Cu-N-5%-RT	Cu-N-5%-400	Cu-N-5%-600
Cu (II) 2p BE (eV)	954.4/934.5	954.6/934.4	954.2/934.0
Cu (I) 2p BE (eV)	952.3/932.5	952.4/932.6	952.3/932.5
Cu LMM Auger KE (eV)	916.1	915.5	915.3
Cu (II) percentage	58%	17%	24%
N 1s BE (eV)	400.4/399.4	400.7/398.9	401.1/398.9
Pyridinic N percentage	67%[a]	88%	80%
Pyrrolic N percentage	33%	12%	20%

[a] Metal-N functionality.

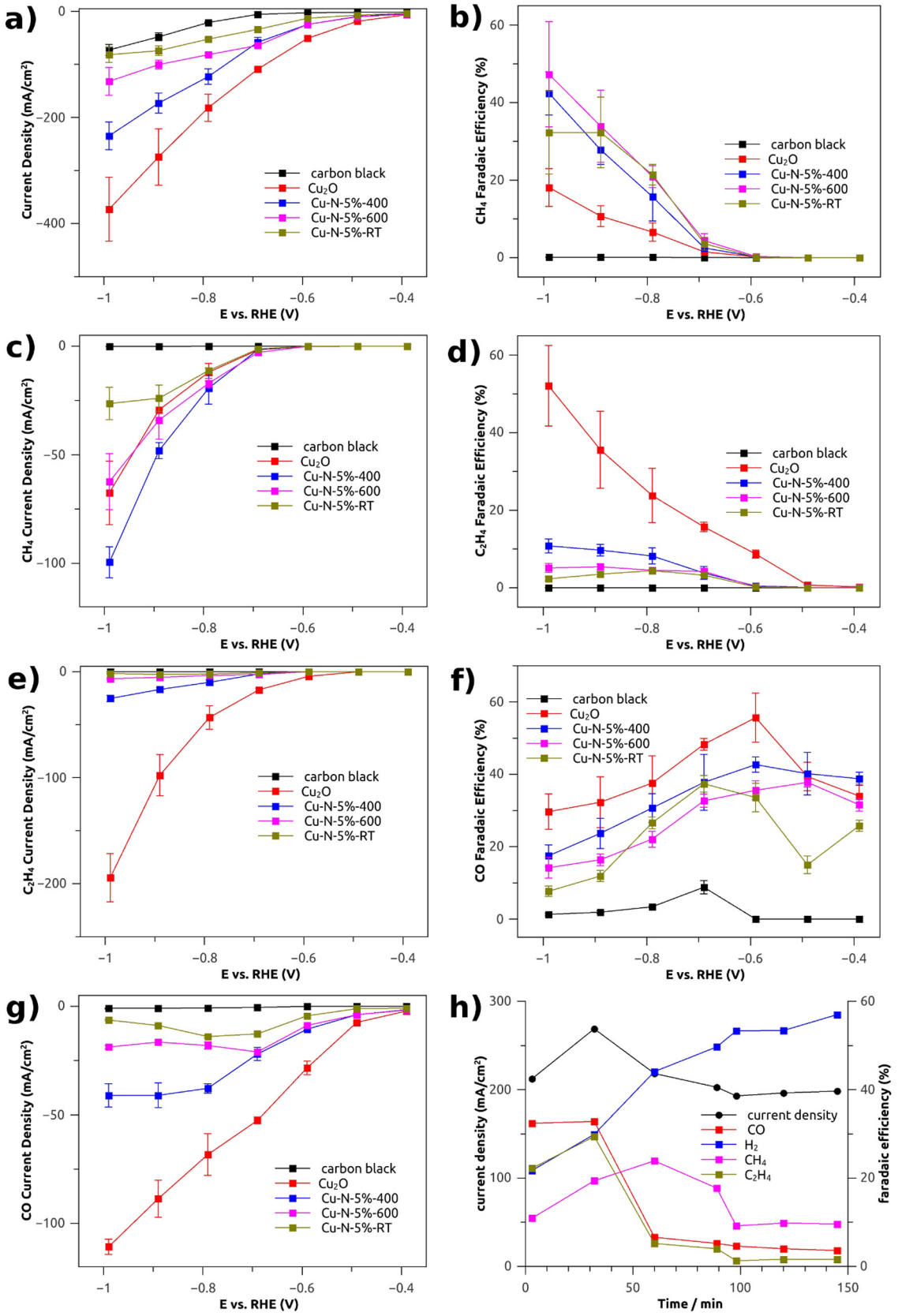

Fig. 3. Total current densities (a), Faradaic efficiencies (b, d, f) and partial current densities (c, e, g) for different CO_2 reduction products (methane – b, c; and ethylene – d, e; CO – f, g) when using the different CuN catalyst and controls. (h) Long term electrolysis performance of Cu-N-5%-400 at − 1.0 V vs. RHE. Electrolysis was conducted in a flow cell with 1 M KOH (aq) as the electrolyte. The flow rates were 7 sc mL/min for CO_2 and 0.5 mL/min for catholyte and anolyte, respectively. Catalyst loading was 1.2 mg/cm^2 for total weight and 0.06–0.16 mg/cm^2 for copper depending on copper weight percentage.

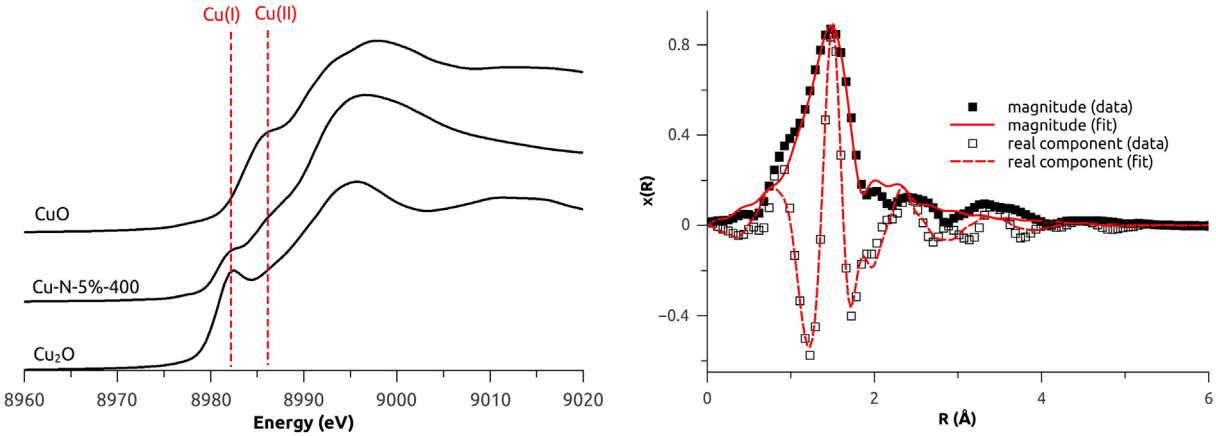

Fig. 4. XANES (left) and EXAFS (right) spectra of the Cu-N-5%-400 catalyst.

and the copper distribution on the post-electrolysis cathode surface was as even as the pre-electrolysis sample (Figs. 5 and S6). These results further support the single-site structure of catalytic copper centers in these catalyst materials. However, copper concentration on cathode surface decreased from 13.2 wt% to 1.83 wt% after electrolysis, which could account for the poor durability performance of the catalyst. Such a sharp concentration drop could be attributed to deposition of inorganic salts (KOH or K_2CO_3) on the electrode surface as well as copper leaching in highly alkaline media.

Carbon dioxide reduction pathways have been explored intensively. Theoretical and experimental studies have suggested the reductive coupling of adsorbed CO species as the crucial step for the production of ethylene and other C2 products [54,55]. Given the presence of a single-site species in the material, we propose that the CC coupling step is strongly disfavored on the catalytic sites, thus C_2H_4 production is suppressed. Our result agrees with the earlier reports that shows that limited size Cu nanoparticles prefer methane production upon the electroreduction of CO_2 [11,18] and is also consistent with predictions. [56]

While copper-based electrocatalysts have attracted the most research interest in the area of CO_2 electroreduction, specifically to C2 hydrocarbons, tuning their selectivity towards a single desired product remains

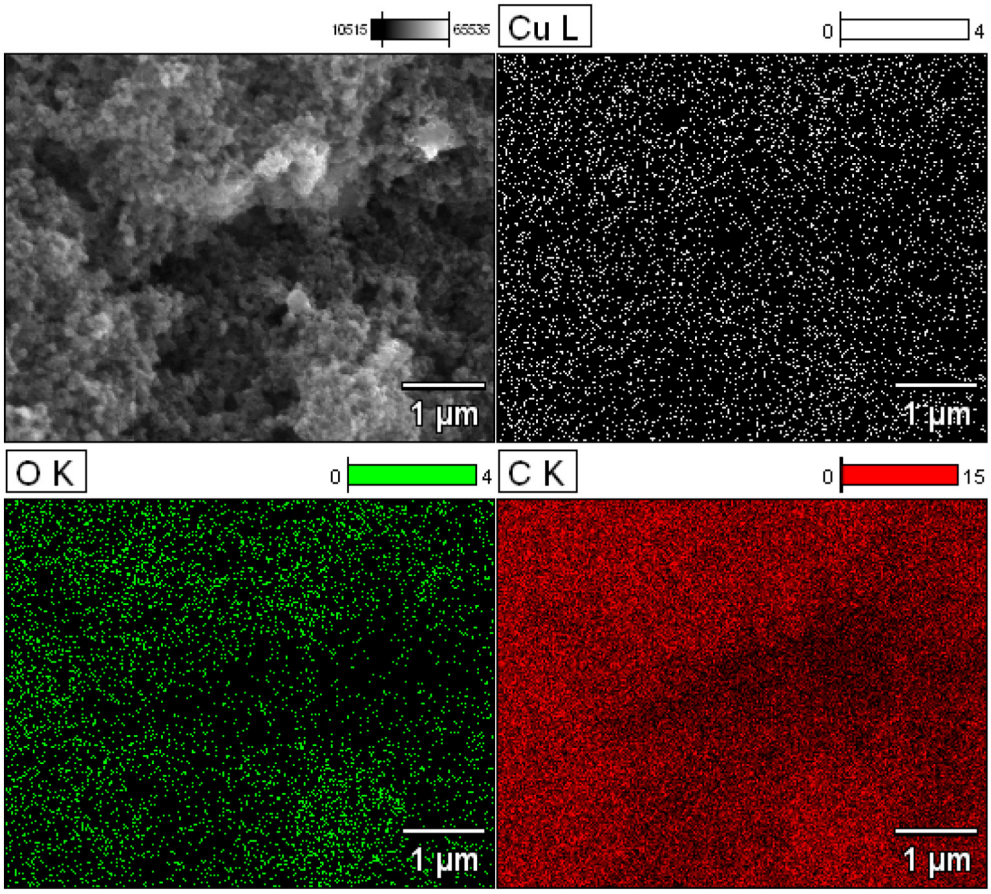

Fig. 5. SEM image and EDX mapping of Cu-N-5%-400 carbon paper electrodes after electrolysis.

challenging. In this report, we developed a single-site catalyst that produce methane with a selectivity as high as 42% via the electroreduction of CO_2 with low Cu usage. Use of these CuN materials represents a new strategy to control the product selectivity in CO_2 reduction. Uncovering the mechanistic details of this unique selectivity will undoubtedly provide insights into design and development of other single-site electrocatalysts, which in turn may lead to improved catalytic properties in CO_2 reduction and other electrochemical reactions.

CRediT authorship contribution statement

Teng Zhang: Conceptualization, Investigation, Writing - original draft. **Sumit Verma:** Conceptualization, Investigation. **Soojeong Kim:** Investigation. **Tim T. Fister:** Investigation, Resources. **Paul J.A. Kenis:** Conceptualization, Resources, Supervision. **Andrew A. Gewirth:** Conceptualization, Resources, Writing - original draft, Supervision.

Declaration of competing interest

The authors declare that they have no known competing financial interests or personal relationships that could have appeared to influence the work reported in this paper.

Acknowledgement

We thank the National Science Foundation (CHE-1309731) for support of this research. The authors also gratefully acknowledge the support of the International Institute for Carbon Neutral Energy Research (WPI-I2CNER), sponsored by the Japanese Ministry of Education, Culture, Sports, Science and Technology.

Appendix A. Supplementary data

Supplementary data to this article can be found online at https://doi.org/10.1016/j.jelechem.2020.113862.

References

[1] https://www.esrl.noaa.gov/gmd/ccgg/trends/global.html.
[2] J. Hansen, P. Kharecha, M. Sato, V. Masson-Delmotte, F. Ackerman, D.J. Beerling, P.J. Hearty, O. Hoegh-Guldberg, S.-L. Hsu, C. Parmesan, J. Rockstrom, E.J. Rohling, J. Sachs, P. Smith, K. Steffen, L. Van Susteren, K. von Schuckmann, J.C. Zachos, PLoS One 8 (2013), e81648.
[3] S. Verma, B. Kim, H. Jhong, S.C. Ma, P.J.A. Kenis, Chemsuschem 9 (2016) 1972–1979.
[4] X.P. Li, P. Anderson, H.R.M. Jhong, M. Paster, J.F. Stubbins, P.J.A. Kenis, Energy Fuel 30 (2016) 5980–5989.
[5] J. Qiao, Y. Liu, F. Hong, J. Zhang, Chem. Soc. Rev. 43 (2014) 631–675.
[6] B. Khezri, A.C. Fisher, M. Pumera, J. Mater. Chem. A 5 (2017) 8230–8246.
[7] D.D. Zhu, J.L. Liu, S.Z. Qiao, Adv. Mater. 28 (2016) 3423–3452.
[8] Y. Hori, K. Kikuchi, S. Suzuki, Chem. Lett. 14 (1985) 1695–1698.
[9] Y. Hori, K. Kikuchi, A. Murata, S. Suzuki, Chem. Lett. 15 (1986) 897–898.
[10] R. Kas, R. Kortlever, A. Milbrat, M.T.M. Koper, G. Mul, J. Baltrusaitis, Phys. Chem. Chem. Phys. 16 (2014) 12194–12201.
[11] K. Manthiram, B.J. Beberwyck, A.P. Alivisatos, J. Am. Chem. Soc. 136 (2014) 13319–13325.
[12] R. Reske, H. Mistry, F. Behafarid, B. Roldan Cuenya, P. Strasser, J. Am. Chem. Soc. 136 (2014) 6978–6986.
[13] F.S. Roberts, K.P. Kuhl, A. Nilsson, Angew. Chem. Int. Ed. 54 (2015) 5179–5182.
[14] A. Loiudice, P. Lobaccaro, E.A. Kamali, T. Thao, B.H. Huang, J.W. Ager, R. Buonsanti, Angew. Chem. Int. Ed. 55 (2016) 5789–5792.
[15] M. Ma, K. Djanashvili, W.A. Smith, Angew. Chem. Int. Ed. 55 (2016) 6680–6684.
[16] Y. Song, R. Peng, D.K. Hensley, P.V. Bonnesen, L. Liang, Z. Wu, H.M. Meyer, M. Chi, C. Ma, B.G. Sumpter, A.J. Rondinone, ChemistrySelect 1 (2016) 6055–6061.
[17] Y. Li, F. Cui, M.B. Ross, D. Kim, Y. Sun, P. Yang, Nano Lett. 17 (2017) 1312–1317.
[18] M.K. Kim, H.J. Kim, H. Lim, Y. Kwon, H.M. Jeong, Electrochim. Acta 306 (2019) 28–34.
[19] M. Watanabe, M. Shibata, A. Kato, M. Azuma, T. Sakata, J. Electrochem. Soc. 138 (1991) 3382–3389.
[20] S. Ishimaru, R. Shiratsuchi, G. Nogami, J. Electrochem. Soc. 147 (2000) 1864–1867.
[21] D. Kim, J. Resasco, Y. Yu, A.M. Asiri, P. Yang, Nat. Commun. 5 (2014) 4948.
[22] X. Guo, Y. Zhang, C. Deng, X. Li, Y. Xue, Y.-M. Yan, K. Sun, Chem. Commun. 51 (2015) 1345–1348.
[23] S. Rasul, D.H. Anjum, A. Jedidi, Y. Minenkov, L. Cavallo, K. Takanabe, Angew. Chem. Int. Ed. 54 (2014) 2146–2150.
[24] S. Zhang, P. Kang, M. Bakir, A.M. Lapides, C.J. Dares, T.J. Meyer, Proc. Natl. Acad. Sci. 112 (2015) 15809–15814.
[25] S. Sarfraz, A.T. Garcia-Esparza, A. Jedidi, L. Cavallo, K. Takanabe, ACS Catal. 6 (2016) 2842–2851.
[26] S. Ma, M. Sadakiyo, M. Heima, R. Luo, R.T. Haasch, J.I. Gold, M. Yamauchi, P.J.A. Kenis, J. Am. Chem. Soc. 139 (2017) 47–50.
[27] G. Yin, H. Abe, R. Kodiyath, S. Ueda, N. Srinivasan, A. Yamaguchi, M. Miyauchi, J. Mater. Chem. A 5 (2017) 12113–12119.
[28] K.W. Frese, J. Electrochem. Soc. 138 (1991) 3338–3344.
[29] M. Le, M. Ren, Z. Zhang, P.T. Sprunger, R.L. Kurtz, J.C. Flake, J. Electrochem. Soc. 158 (2011) E45–E49.
[30] D. Ren, Y. Deng, A.D. Handoko, C.S. Chen, S. Malkhandi, B.S. Yeo, ACS Catal. 5 (2015) 2814–2821.
[31] R.J. Haines, R.E. Wittrig, C.P. Kubiak, Inorg. Chem. 33 (1994) 4723–4728.
[32] R. Angamuthu, P. Byers, M. Lutz, A.L. Spek, E. Bouwman, Science 327 (2010) 313.
[33] Z. Weng, J. Jiang, Y. Wu, Z. Wu, X. Guo, K.L. Materna, W. Liu, V.S. Batista, G.W. Brudvig, H. Wang, J. Am. Chem. Soc. 138 (2016) 8076–8079.
[34] Y. Chen, S. Ji, C. Chen, Q. Peng, D. Wang, Y. Li, Joule 2 (2018) 1242–1264.
[35] T. Sun, L. Xu, D. Wang, Y. Li, Nano Res. 12 (2019) 2067–2080.
[36] R.L. Cook, R.C. Macduff, A.F. Sammells, J. Electrochem. Soc. 134 (1987) 2375–2376.
[37] J.J. Kim, D.P. Summers, K.W. Frese, J. Electroanal. Chem. Interfacial Electrochem. 245 (1988) 223–244.
[38] D.W. Dewulf, T. Jin, A.J. Bard, J. Electrochem. Soc. 136 (1989) 1686–1691.
[39] Y. Hori, A. Murata, R. Takahashi, Journal of the Chemical Society, Faraday Transactions 1: Physical Chemistry in Condensed Phases 85 (1989) 2309–2326.
[40] R.L. Cook, R.C. Macduff, A.F. Sammells, J. Electrochem. Soc. 137 (1990) 607–608.
[41] T.T.H. Hoang, S. Ma, J.I. Gold, P.J.A. Kenis, A.A. Gewirth, ACS Catal. 7 (2017) 3313–3321.
[42] W. Tang, A.A. Peterson, A.S. Varela, Z.P. Jovanov, L. Bech, W.J. Durand, S. Dahl, J.K. Nørskov, I. Chorkendorff, Phys. Chem. Chem. Phys. 14 (2012) 76–81.
[43] H. Mistry, A.S. Varela, C.S. Bonifacio, I. Zegkinoglou, I. Sinev, Y.-W. Choi, K. Kisslinger, E.A. Stach, J.C. Yang, P. Strasser, B.R. Cuenya, Nat. Commun. 7 (2016) 12123.
[44] Y. Zhao, C. Wang, G.G. Wallace, J. Mater. Chem. A 4 (2016) 10710–10718.
[45] T.V. Magdesieva, I.V. Zhukov, D.N. Kravchuk, O.A. Semenikhin, L.G. Tomilova, K.P. Butin, Russ. Chem. Bull. 51 (2002) 805–812.
[46] S. Kaneco, K. Iiba, S. Suzuki, K. Ohta, T. Mizuno, J. Phys. Chem. B 103 (1999) 7456–7460.
[47] C.-T. Dinh, T. Burdyny, M.G. Kibria, A. Seifitokaldani, C.M. Gabardo, F.P. García de Arquer, A. Kiani, J.P. Edwards, P. De Luna, O.S. Bushuyev, C. Zou, R. Quintero-Bermudez, Y. Pang, D. Sinton, E.H. Sargent, Science 360 (2018) 783.
[48] Y. Hori, I. Takahashi, O. Koga, N. Hoshi, J. Phys. Chem. B 106 (2002) 15–17.
[49] I. Takahashi, O. Koga, N. Hoshi, Y. Hori, J. Electroanal. Chem. 533 (2002) 135–143.
[50] Y. Hori, I. Takahashi, O. Koga, N. Hoshi, J. Mol. Catal. A Chem. 199 (2003) 39–47.
[51] K. Artyushkova, B. Kiefer, B. Halevi, A. Knop-Gericke, R. Schlogl, P. Atanassov, Chem. Commun. 49 (2013) 2539–2541.
[52] P.R. Sarode, G. Sankar, C.N.R. Rao, Proceedings of the Indian Academy of Sciences - Chemical Sciences 92 (1983) 527–542.
[53] A. Sharma, M. Varshney, J. Park, T.-K. Ha, K.-H. Chae, H.-J. Shin, RSC Adv. 5 (2015) 21762–21771.
[54] R. Kortlever, J. Shen, K.J.P. Schouten, F. Calle-Vallejo, M.T.M. Koper, The Journal of Physical Chemistry Letters 6 (2015) 4073–4082.
[55] E. Pérez-Gallent, M.C. Figueiredo, F. Calle-Vallejo, M.T.M. Koper, Angew. Chem. Int. Ed. 56 (2017) 3621–3624.
[56] M.J. Cheng, E.L. Clark, H.H. Pham, A.T. Bell, M. Head-Gordon, ACS Catal. 6 (2016) 7769–7777.